

REPORT DOCUMENTATION PAGE				Form Approved OMB No. 0704-0188	
The public reporting burden for this collection of information is estimated to average 1 hour per response, including the time for reviewing instructions, searching existing data sources, gathering and maintaining the data needed, and completing and reviewing the collection of information. Send comments regarding this burden estimate or any other aspect of this collection of information, including suggestions for reducing the burden, to the Department of Defense, Executive Services and Communications Directorate (0704-0188). Respondents should be aware that notwithstanding any other provision of law, no person shall be subject to any penalty for failing to comply with a collection of information if it does not display a currently valid OMB control number.					
PLEASE DO NOT RETURN YOUR FORM TO THE ABOVE ORGANIZATION.					
1. REPORT DATE (DD-MM-YYYY) 14-02-2006		2. REPORT TYPE Journal Article (refereed)		3. DATES COVERED (From - To)	
4. TITLE AND SUBTITLE Transport Variability Across the Korea/Tsushima Strait and the Tsushima Island Wake				5a. CONTRACT NUMBER	
				5b. GRANT NUMBER	
				5c. PROGRAM ELEMENT NUMBER PE0601153N	
6. AUTHOR(S) Teague, W.J., Hwang, P.A., Jacobs, G.A., Book, J.W., Perkins, H.T.				5d. PROJECT NUMBER	
				5e. TASK NUMBER	
				5f. WORK UNIT NUMBER 73-7607-02-5	
7. PERFORMING ORGANIZATION NAME(S) AND ADDRESS(ES) Naval Research Laboratory Oceanography Division Stennis Space Center, MS 39529-5004				8. PERFORMING ORGANIZATION REPORT NUMBER NRL/JA/7330-02-0053	
9. SPONSORING/MONITORING AGENCY NAME(S) AND ADDRESS(ES) Office of Naval Research 800 N. Quincy St. Arlington, VA 22217-5660				10. SPONSOR/MONITOR'S ACRONYM(S) ONR	
				11. SPONSOR/MONITOR'S REPORT NUMBER(S)	
12. DISTRIBUTION/AVAILABILITY STATEMENT Approved for public release, distribution is unlimited.					
13. SUPPLEMENTARY NOTES <i>U.S. Government actions; ALL - Work of the U.S. Government.</i>					
14. ABSTRACT Transport variations are calculated across the Korea/Tsushima Strait using continuous current measurements made between May 1999 and March 2000. 12 bottom-mounted acoustic Doppler current profilers provide velocity profiles along 2 sections: one section (south line) at the strait entrance southwest (upstream) of Tsushima Island and the other section (north line) at the strait exit northeast (downstream) of Tsushima Island. Transport variations across the strait are large, particularly in the lee of Tsushima Island where a countercurrent commonly exists. The Tsushima Current transport, averaging 2.65 Sverdrups (Sv) is split into 2 cores by Tsushima Island, which divides the strait into eastern and western channels. Transport in the western channel is 23% higher than in the eastern channel over the measurement period. Some seasonality in transport variability is observed for both the western and eastern channels. Transports are largest in fall and smallest during winter. The single-velocity core, observed upstream of Tsushima Island, is estimated to split directly behind Tsushima Island over and aperture of about 31 km along the south line. A wake zone that averages 40 km in width is observed downstream of Tsushima Island and appears to follow island-wake-zone dynamics. Reynolds numbers can range from 22 to 90 in the wake zone, and eddy shedding can occur throughout the year.					
15. SUBJECT TERMS transport variations, channel, barotropic, moorings,					
16. SECURITY CLASSIFICATION OF:			17. LIMITATION OF ABSTRACT  UL	18. NUMBER OF PAGES 18	19a. NAME OF RESPONSIBLE PERSON William Teague
a. REPORT Unclassified	b. ABSTRACT Unclassified	c. THIS PAGE Unclassified			19b. TELEPHONE NUMBER (Include area code) (228) 688-4734

20060605026

## PUBLICATION OR PRESENTATION RELEASE REQUEST

Pubkey: 3192

NRLINST 5600.2

1. REFERENCES AND ENCLOSURES	2. TYPE OF PUBLICATION OR PRESENTATION	3. ADMINISTRATIVE INFORMATION
Ref: (a) NRL Instruction 5600.2 (b) NRL Instruction 5510.40D	( ) Abstract only, published ( ) Book ( ) Conference Proceedings (refereed) ( ) Invited speaker (X) Journal article (refereed) ( ) Oral Presentation, published ( ) Other, explain	STRN <u>NRL/JA/7330-02-53</u> Route Sheet No. <u>7330/</u> Job Order No. _____ Classification <u>X</u> U _____ C Sponsor _____ approval obtained <u>X</u> yes _____ no
Encl: (1) Two copies of subject paper (or abstract)	( ) Abstract only, not published ( ) Book chapter ( ) Conference Proceedings (not refereed) ( ) Multimedia report ( ) Journal article (not refereed) ( ) Oral Presentation, not published	

## 4. AUTHOR

Title of Paper or Presentation

Transport Variability Across the Korea/Tsushima Strait and the Tsushima Island Wake

Author(s) Name(s) (First, MI, Last), Code, Affiliation if not NRL

William J. Teague, Paul A. Hwang, Gregg A. Jacobs, Jeffrey W. Book, Henry T. Perkins

It is intended to offer this paper to the \_\_\_\_\_

(Name of Conference)

(Date, Place and Classification of Conference)

and/or for publication in Deep Sea Research, Unclassified

(Name and Classification of Publication)

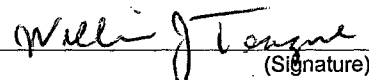
(Name of Publisher)

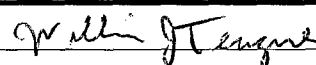
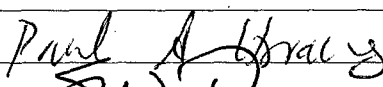
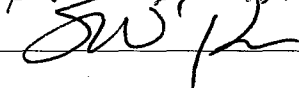

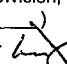

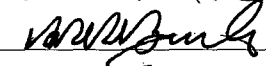
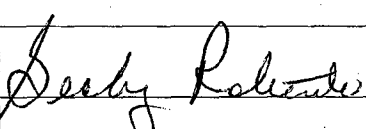
After presentation or publication, pertinent publication/presentation data will be entered in the publications data base, in accordance with reference (a).

It is the opinion of the author that the subject paper (is \_\_\_\_\_) (is not X) classified, in accordance with reference (b).This paper does not violate any disclosure of trade secrets or suggestions of outside individuals or concerns which have been communicated to the Laboratory in confidence. This paper (does \_\_\_\_\_) (does not X) contain any militarily critical technology.This subject paper (has \_\_\_\_\_) (has never X) been incorporated in an official NRL Report.

William J. Teague, 7332

Name and Code (Principal Author)


  
(Signature)

5. ROUTING/APPROVAL			
CODE	SIGNATURE	DATE	COMMENTS
Author(s) Teague	X 	3/8/02	
Section Head Hwang		3/8/02	
Branch Head Steven W. Payne, 7330		3/11/02	
Division Head William J. Jobst, 7300		3/11/02	1. Release of this paper is approved. 2. To the best knowledge of this Division, the subject matter of this paper (has _____) (has never <u>X</u> ) been classified. 
Security, Code 7030.1		3/12/02	1. Paper or abstract was released. 2. A copy is filed in this office. @SSC-103-0
Office of Counsel, Code 1008.3		3/21/02	
ADOR/Director NCST E.O. Hartwig, 7000			
Public Affairs (Unclassified/ Unlimited Only), Code 7030.4		3/18/02	
Division, Code			
Author, Code			



## Transport variability across the Korea/Tsushima Strait and the Tsushima Island wake

W.J. Teague\*, P.A. Hwang, G.A. Jacobs, J.W. Book, H.T. Perkins

*Naval Research Laboratory, Stennis Space Center, MS 39529, USA*

Received 19 July 2002; received in revised form 29 June 2003; accepted 25 July 2003

Available online 15 July 2005

### Abstract

Transport variations are calculated across the Korea/Tsushima Strait using continuous current measurements made between May 1999 and March 2000. Twelve bottom-mounted acoustic Doppler current profilers provide velocity profiles along two sections: one section (south line) at the strait entrance southwest (upstream) of Tsushima Island and the other section (north line) at the strait exit northeast (downstream) of Tsushima Island. Transport variations across the strait are large, particularly in the lee of Tsushima Island where a countercurrent commonly exists. The Tsushima Current transport, averaging 2.65 Sverdrups (Sv) ( $1 \text{ Sv} = 10^6 \text{ m}^3 \text{ s}^{-1}$ ), is split into two cores by Tsushima Island, which divides the strait into eastern and western channels. Transport in the western channel is 23% higher than in the eastern channel over the measurement period. Some seasonality in transport variability is observed for both the western and eastern channels. Transports are largest in fall and smallest during winter. The single-velocity core, observed upstream of Tsushima Island, is estimated to split directly behind Tsushima Island over an aperture of about 31 km along the south line. A wake zone that averages 40 km in width is observed downstream of Tsushima Island and appears to follow island-wake-zone dynamics. Reynolds numbers can range from 22 to 90 in the wake zone, and eddy shedding can occur throughout the year.

Published by Elsevier Ltd.

### 1. Introduction

The Tsushima Current flows from the East China Sea to the Japan/East Sea via the Korea/Tsushima Strait. This current is important in the

transfer of heat, salt, and nutrients into the Japan/East Sea. Thus, volume transports and variability of the Tsushima Current across the strait are of high interest. Throughout the last several decades, many current observations have been made to determine the volume transport and spatial structure of the Tsushima Current in the Korea/Tsushima Strait (Mizuno et al., 1989; Egawa et al., 1993; Katoh et al., 1996; Isobe et al., 2002). The

\*Corresponding author. Tel.: +1 228 688 4734;

fax: +1 228 688 5997.

E-mail address: teague@nrlssc.navy.mil (W.J. Teague).

major current features in the strait are the inflow of the Tsushima Current from the East China Sea, inflow of the Cheju Current, which is composed primarily of waters of Kuroshio origin through the Cheju Strait (Chang et al., 2000; Lie et al., 2000), a counter flow on the east side of Tsushima Island (Miita and Ogawa, 1984; Egawa et al., 1993), and a splitting of the Tsushima Current around Tsushima Island into at least two branches (Isobe, 1997). In the three-branch scenario, the first branch is controlled by the bottom topography and flows through the eastern channel along the Japanese coast as the Nearshore Branch (Yoon, 1982b). The second and third branches originate in the western channel and bifurcate into two branches downstream (Katoh, 1994). The second or middle branch, also suggested in the historical interpretation by Suda and Hidaka (1932) and Uda (1934), flows eastward as the offshore branch. The third branch flows northward along the eastern coast of Korea as the East Korean Warm Current (Yoon, 1982a).

Despite the many measurements of currents by direct and indirect methods across the Korea/Tsushima Strait, the structure of the Tsushima Current is still not well known. Long-term measurements of currents are very difficult to make because of intense fishing and trawling (Kawatate et al., 1988). Therefore, such measurements are relatively scarce. Short-term measurements have shown that strong low-frequency currents exist together with strong tidal currents in the strait (Mizuno et al., 1989; Egawa et al., 1993; Isobe et al., 1994; Katoh et al., 1996). Tidal currents with speeds approaching 50 cm/s embedded in total currents of 100 cm/s have been reported by Isobe et al. (1994). Tides have been a major problem in the direct current measurements made using ship-mounted acoustic Doppler current profilers (ADCPs), where ship motions and tides are often a large source of error. Currents have been measured indirectly from hydrographic data using the geostrophic method (Yi, 1966) and also have been deduced from sea-level differences among tidal stations along the Korean and Japanese coasts (Yi, 1970; Kawabe, 1982; Toba et al., 1982). However, it is difficult to estimate more than the baroclinic component of the

geostrophic flow over shallow continental shelves since an absolute velocity reference level is not easily measured. Realistic currents estimated through geostrophic calculations also depend upon the synopticity of the stations and the absence of ageostrophic currents, both of which are problematic assumptions on the shelf. Sea-level differences just provide an estimate of the total barotropic flow across the strait, but there are often difficulties in the absolute referencing of the tide gauges. In general, the currents in the strait are thought to exhibit considerable variation in current velocity (Egawa et al., 1993).

Transports variations across the east and west channels of the Korea/Tsushima Strait are not well determined in either channel. Concurrent measurements of transports in both channels are extremely rare. Historically, the seasonal variations of the currents, and hence transports, are thought to be large. According to studies using sea-level differences across the western channel, currents in the western channel have high variability on a seasonal cycle, with transport at a maximum in summer and fall, and at a minimum in winter and spring (Kawabe, 1982; Toba et al., 1982). A similar study by Mizuno et al. (1989) could not identify a seasonal cycle in the eastern channel. Likewise, a study by Egawa et al. (1993) using ADCP data from ships of opportunity found little seasonal variability of the currents in the eastern channel. From hydrographic measurements and the geostrophic method, Yi (1966) found mean annual volume transports for the western and eastern channels of 0.9 and 0.3 Sv, respectively. A higher value of 1.3 Sv for the mean transport of the western channel was found by Lee (1974) through direct current observations from an anchored ship. The higher value is attributed to a barotropic transport. Larger values of transport, 1.8 Sv for the western channel and 1.6 Sv for the eastern channel, were found by Miita (1976) using data from current meters suspended from anchored ships over a period of just a few days. A study by Kaneko et al. (1991) suggests that transports are 2–3 times larger in the western channel than in the eastern channel where transports of 0.7 Sv are found. Kawabe (1982) also found larger transports in the western channel. Katoh (1993) found that

the transport through the eastern channel fluctuates considerably, ranging from about 0.5 Sv to more than 1.5 Sv. In a study by Isobe et al. (1994), total volume transports are calculated about every 2 months from 1990 to 1991 using a ship-towed ADCP. They found total volume transport across the strait is at a maximum of about 5.6 Sv in September, while only about 1.0 Sv during the rest of the year. Most of the transport was concentrated in the region near the Korea coast, and hence fluctuations in the transport near Korea was responsible for the seasonal variability, though small, across the strait. These short-term measurements have suggested a wide range of variability in the transport distribution across the Korea/Tsushima Strait.

ADCP moorings using trawl-resistant bottom mounts (TRBMs) can now be deployed for long-term measurements of currents for time periods approaching a year or longer (Perkins et al., 2000a). Here, transports are examined using current measurements from 12 bottom-mounted ADCPs deployed on two lines located downstream (north section) and upstream (south section) of Tsushima Island (Fig. 1). Total volume transports of the Tsushima Current have been reported using these data by Jacobs et al. (2001) and Teague et al. (2002). They estimated total transports of 2.9 Sv for May–September 1999 and 2.7 Sv for May 1999–March 2000, respectively, but did not estimate transports through the west and east channels. Highest non-tidal velocities, often exceeding 70 cm/s, are found on the north section near Korea. Highest non-tidal velocities in the south section are about 50 cm/s and are found near mid-strait. The north section, is characterized by strong spatial variability, but in the mean consists of two streams, one on each side of the strait. Between the two high-velocity streams is a region of highly variable flow with a weak mean, presumably due to the island wake behind Tsushima Island (discussed in Section 5).

Transports across the entire Korea/Tsushima Strait and in the eastern and western channels are calculated here using long-term velocity measurements made along two ADCP sections located upstream and downstream of Tsushima Island between May 1999 and March 2000. In addition,

the wake zone behind Tsushima Island is discussed. Current profiles measured by bottom moored ADCPs over long time periods are ideal for answering questions pertaining to currents and transports, which have never been adequately addressed due to the difficulty in making such measurements.

## 2. Instrumentation

Twelve moorings were deployed along two lines, northeast (downstream) and southwest (upstream) of Tsushima Island, in the Korea/Tsushima Strait during May 1999 (Fig. 1). The line southwest of Tsushima is referred to as the south line (S1–S6) and the line northeast of Tsushima as the north line (N1–N6). Geographical positions, depths, and times for each of the moorings are tabulated in Teague et al. (2002). Each deployed package contained an ADCP housed in a TRBM. Nine of the deployments were based on a new type of TRBM known as Barnys after their barnacle-like shape (Perkins et al., 2000b). The Barnys were developed by SACLANT Center in collaboration with the Naval Research Laboratory (NRL). The remaining TRBMs, at sites N2, N3, and S5, were of a different design developed at the Naval Oceanographic Office (Teague et al., 1998). In general, both types of mounts are shallow dome-shaped enclosures that rest upon the bottom. The exposed side of the dome is relatively smooth in order to minimize snagging by fishing nets and lines.

The Barny mounts were equipped with RD Instruments Workhorse ADCPs operating at 300 kHz. The TRBMs from the Naval Oceanographic Office were equipped with RD Instruments Narrowband ADCPs operating at 150 kHz. All packages contained EdgeTech Model 8202 acoustic releases for location and recovery. The instrument, protected within the mount, rest about 0.5 m above the ocean bottom. The ADCPs were set up to provide current profiles with an accuracy of 1 cm/s over nearly the full water column. Depth resolution is 2 m at S1, S2, and N2, and 4 m for the other ADCPs. Profiles of  $u$  (east–west) and  $v$  (north–south) components of

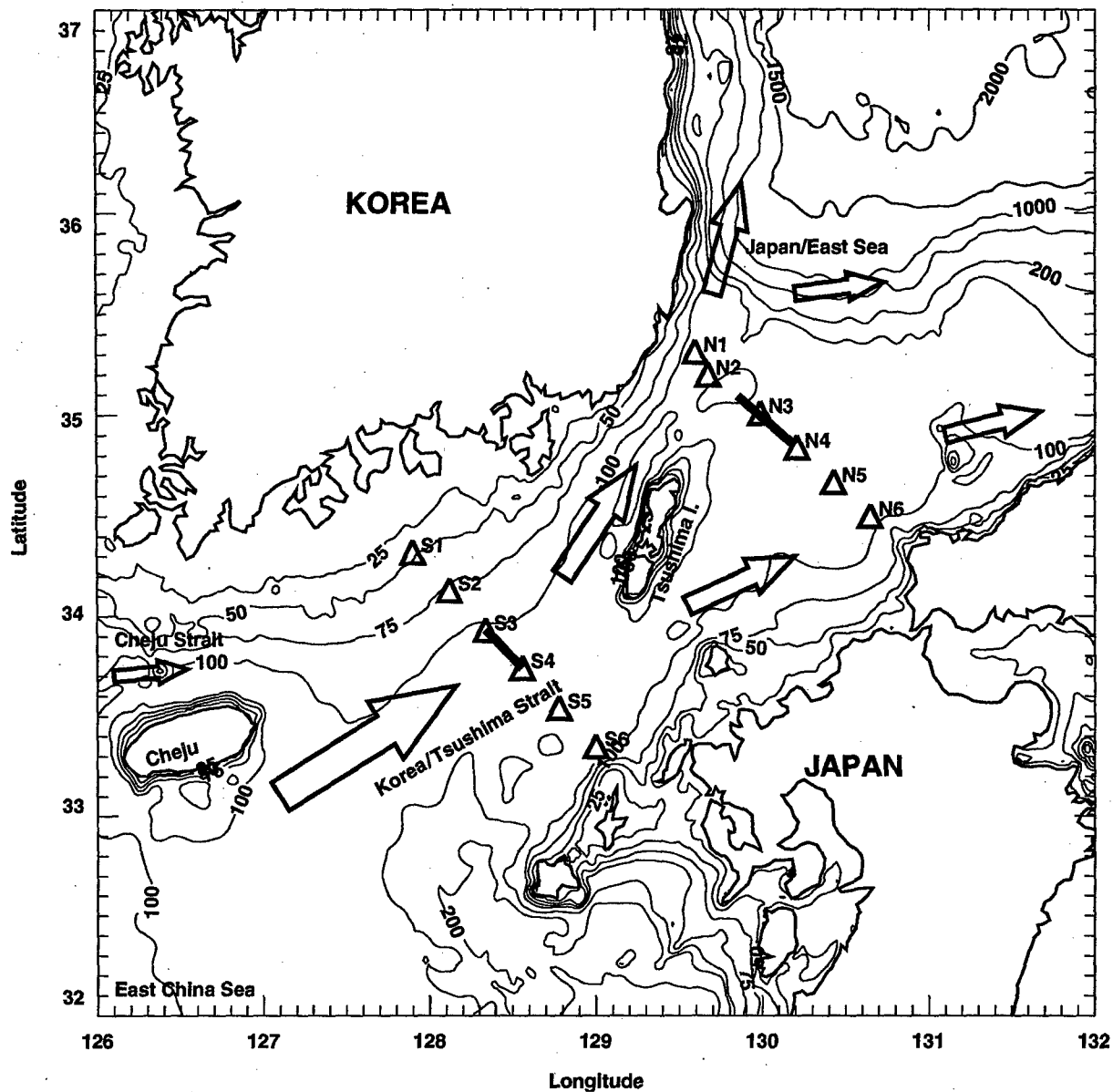


Fig. 1. ADCP mooring locations, bathymetry (m), and simplified current flow are shown. The Tsushima Current from the East China Sea and the Cheju Current through the Cheju Strait provide the inflow into the Korea/Tsushima Strait. The inflow is split into western and eastern channels by Tsushima Island and is generally believed to form up to three branches in the Japan/East Sea. The heavy bar on the south line (S1–S6) indicates the section where the Tsushima Current splits into the western and eastern channels. The heavy bar on the north line (N1–N6) indicates the highly variable, low-transport, island-wake section. Bathymetry is from a 1-min resolution data set available from the Laboratory for Coastal and Ocean Dynamics Studies, Sung Kyun Kwan University (Choi, 1999) and the contour levels shown are: 25, 50, 75, 100, 150, 200, 500, 1000, 1500, and 2000 m.

velocity were recorded at 30-min intervals except at 15-min intervals at S5, N2, and N3. Scraps of nets as well as evidence of trawl scrapings were

found on the moorings at instrument retrieval. The tides and currents are analyzed in Teague et al. (2001, 2002).

### 3. Transport calculation

Details of the transport calculation and an error analysis are provided by Jacobs et al. (2001). Briefly, an optimal interpolation (OI) scheme (Bretherton et al., 1976; Lorenc, 1981) is used to interpolate the ADCP observations horizontally and vertically along each mooring section. The solution along each mooring line is derived separately, and the velocities are interpolated at each time independent of other time points. The horizontal length scales, based on the correlation of the velocity time series with the velocity time series at neighboring ADCP moorings and the assumption that the horizontal-distance-lagged correlation function is Gaussian, are between 15 and 30 km at each depth level for each mooring. The Rossby Radius of deformation is 18 km (Cho and Kim, 1998), and the width of the current cores observed by ship ADCP is between 28 and 37 km (Kato, 1993). Thus, the horizontal length scales obtained here are in agreement with theoretical and previously observed scales. Since average spacing between moorings is 25 km, these data can resolve current features on the typically observed horizontal scales. However, current features with spatial scales smaller than the instrument spacing do occur, and these features may not be resolved. In particular, such a problem area is located near the western end of the north section, where intense coastal currents are surmised to occur just off Korea (Miita and Ogawa, 1984; Tawara and Fujiwara, 1985; Egawa et al., 1993). Narrow currents can also be realized between moorings as have been observed by high-resolution snapshots of currents across the strait obtained by a ship-mounted ADCP (Isobe et al., 1994). The interpolation scheme applied here simply extrapolates the velocity value at the mooring to the coast. Thus, transports along the northern mooring line are underestimated when intensified coastal currents occur. The vertical length scales are computed similarly and are about 20 m near the bottom and decrease toward the surface. Transports are also underestimated when currents are surface-intensified. Transport estimate errors based on the horizontal and vertical length scales are about 0.5 Sv.

For analyses of the low-frequency current, currents near the tidal semi-diurnal and diurnal frequencies are removed from the ADCP records by using a low-pass filter with a 40-h cutoff frequency. Velocities are then rotated ( $42.5^\circ$ ) to obtain the along strait velocity which is approximately normal to the mooring lines. Velocities, at 12-h resolution, are interpolated to a 5-km horizontal grid resolution and a 4-m vertical grid resolution. The total transport across each line is the integral over the cross-sectional area of the velocity normal to section.

### 4. Transport distribution across the strait

Velocity distributions are highly variable across the strait. The temporal evolution of the daily mean velocity profiles at the moorings upstream and downstream of Tsushima Island are presented in Figs. 2 and 3, respectively. Velocities are higher from May to November than from December to March. Higher velocities along the south line are found at S2, S3, and S4. The high-velocity core shifts northward towards Korea from August to November. Counter-flows that extend to near-bottom occur between October and December at S6 and in January at S1. Velocities are most intense along the north line from September to November at N1 and N2. A counter flow is observed from May to December at N3 and from August to November at N4. Velocities are generally lower at N5 and N6 than at N1 and N2. The highly variable velocities suggest a pulsing or oscillating flow field.

Transports averaged over the entire measurement period of about a year are shown for each grid cell for the south line in Fig. 4 and for the north line in Fig. 5. A single, high-transport core is apparent near mid-strait in the south line and extends almost to the bottom. Transports then decrease towards the coasts of Korea and Japan. The single core on the south line splits into two cores across the north line, concentrated along the Korea and Japan coasts, and very likely forms the East Korean Warm Current and Nearshore Branch, respectively. Weakest transport is observed in the middle of the north line and a mean

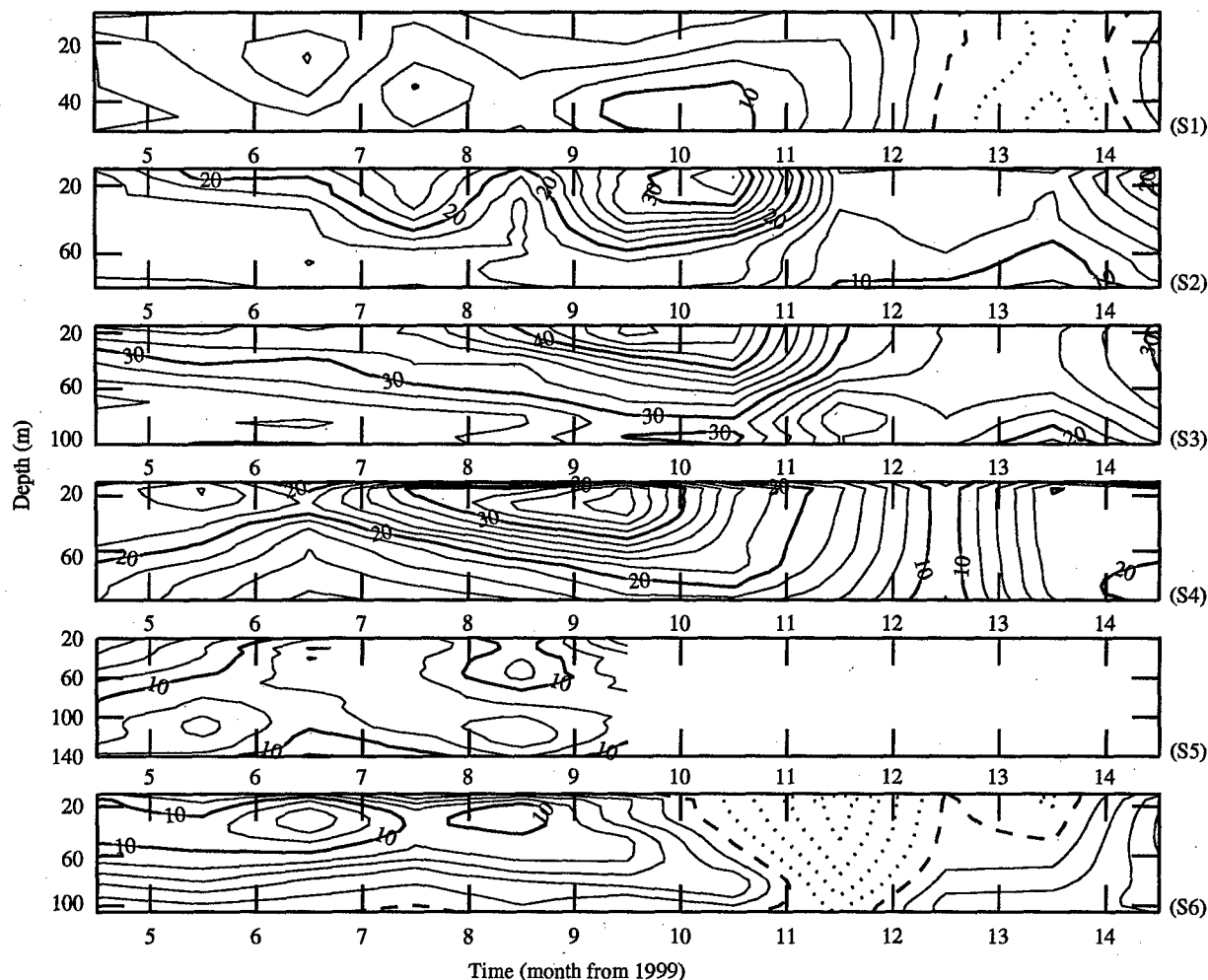


Fig. 2. The temporal evolution of the vertical profiles of the daily mean velocity at the moorings upstream (south line) of Tsushima Island. Dotted contour lines are negative velocities, solid contour lines are positive velocities, and dashed contour lines are zero velocities. Month 5 corresponds to May 1999, and month 14 corresponds to February 2000.

southwestern counter flow is observed near mid-strait. Large transport regions are located near the coasts, with the largest found off Korea. If the Offshore Branch is present during our measurement period, it could branch from either the Nearshore Branch or the East Korean Warm Current further downstream.

The total time-varying transports across the north and south sections is the integral over the cross-sectional area of the interpolated along-strait velocity (Fig. 6). The seasonal signal in the transport shows maximum transport of about

5.5 Sv in October and minimum transport less than 0.5 Sv in December–January. The time average transports for May 1999–March 2000 are 2.65 Sv across south line and 2.38 Sv across the north line, with standard deviations of about 0.9 Sv for both lines. The smaller transport value for the north line is likely due to the omission of high-velocity currents near the coasts and outside the coverage of the mooring lines. Surface intensification of currents outside of the ADCP range also could have resulted in lower calculated transport values. The time-varying total integrated



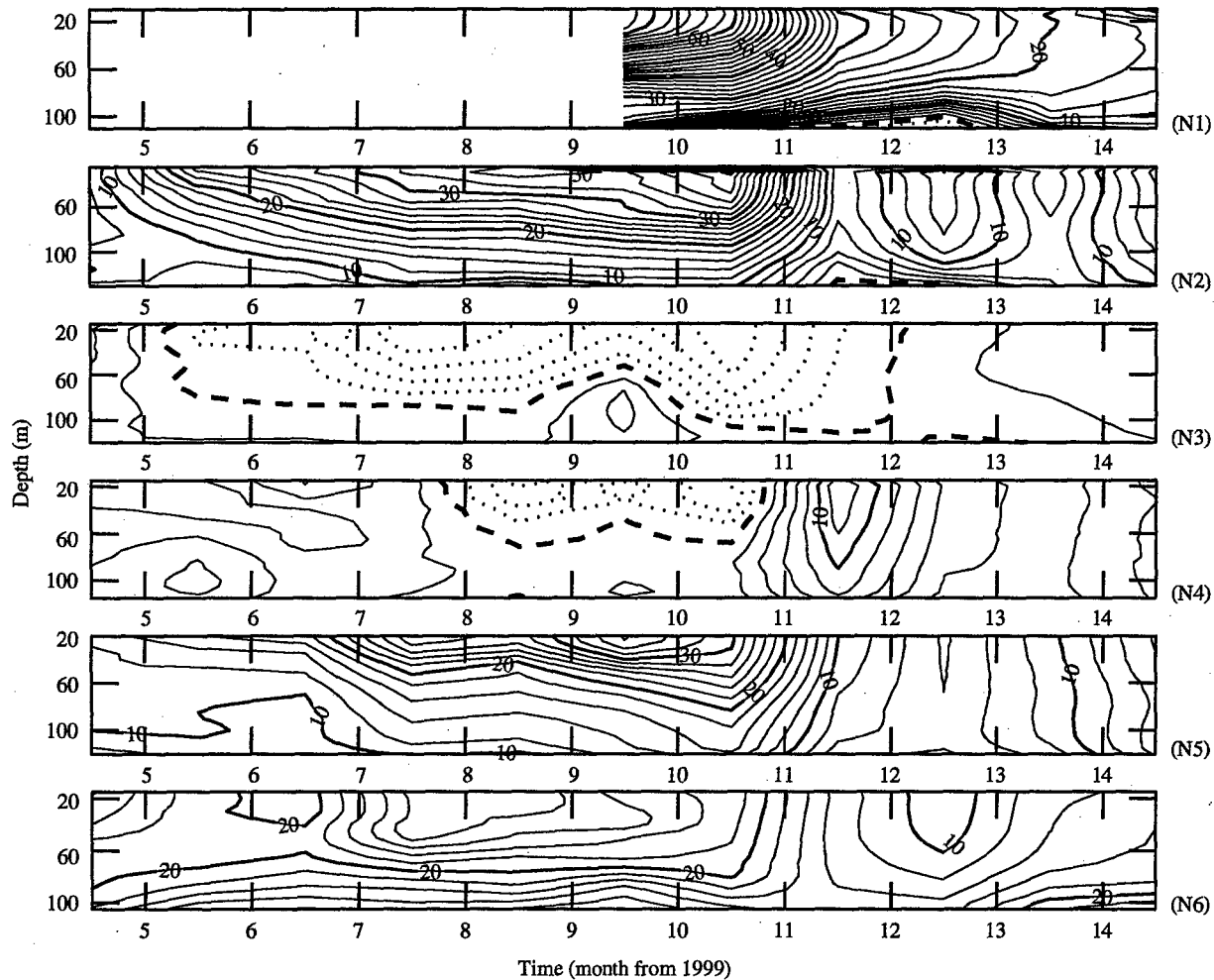


Fig. 3. As in Fig. 2 but for the moorings downstream (north line) of Tsushima Island.

transports across the strait using these measurements have been discussed by Jacobs et al. (2001) and by Teague et al. (2001).

Transport distribution as a function of depth across the Korea/Tsushima Strait is illustrated through the transports measured at the southern line. Normalized cumulative transports versus depth for the southern line are shown for each month and for the 11-month average in Fig. 7. The shapes of the curves describing the monthly transport distributions over depth are very similar throughout the year. Approximately 53% of the average total cumulative transport across the strait is contained in the upper 50 m of the water

column, and 89% is contained in the upper 100 m of the water column. About 11% of the transport is found at depths greater than 100 m. The monthly distributions are most different for February and October, where 50% of the average monthly cumulative transports are contained in the upper 56 and 43 m, respectively. Cumulative transport distributions for July–November are biased toward the shallower depths while the distributions in December–June are biased towards the deeper depths. The relationship of the average transport with depth (darker line in Fig. 7) can be closely approximated using a second degree polynomial curve fitted through the data using a

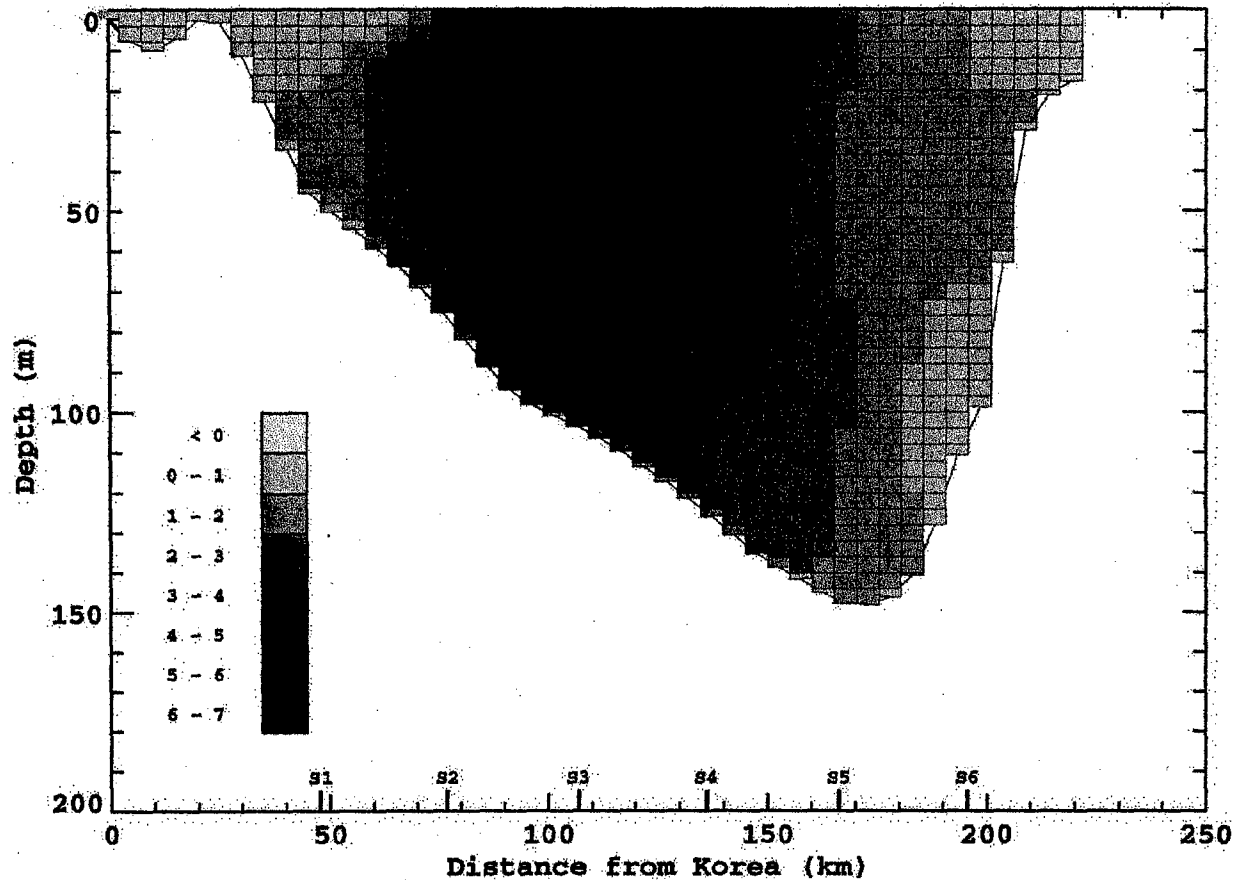


Fig. 4. Transports averaged over May 1999–March 2000 are shown for the south line. Units are  $10^3 \text{ m}^3 \text{ s}^{-1}$  or  $1 \times 10^{-3} \text{ Sv}$ . Each grid square is approximately 5 km across strait by 4 m in depth, except near the bottom where the depth dimension may be less. Positions of moorings, S1–S6, are indicated on the x-axis.

least-squares method. The resulting approximation for cumulative transport,  $T^z$ , is

$$T^z = az^2 + bz + c, \quad (1)$$

where  $a = -4.312 \times 10^{-5}$ ,  $b = 1.340 \times 10^{-2}$ , and  $c = 2.783 \times 10^{-2}$ . The standard deviation of the observations with the fitted values is  $9.229 \times 10^{-3}$ . The larger slope of the cumulative transport versus depth in October than in February is indicative of relatively higher current velocities and thus larger transport in the upper water column. The larger curvature of the cumulative transport distribution over depth for October is related to a larger depth dependence of velocity. In February, the velocities and transports are highly homogeneous over depth.

Transport through the Korea/Tsushima Strait is split by Tsushima Island into western and eastern channels. There have not been long-term or concurrent estimates of transport in the western and eastern channels of the Korea/Tsushima Strait prior to the measurements discussed here. The current split downstream of Tsushima Island likely varies in location over time. An estimate for the location of the transport split along the north line can be made using the average cumulative transport distribution over the year as a function of distance from Korea (Fig. 8). Very low transport is found almost directly downstream of Tsushima Island throughout the year. On average, transport is near zero in a zone approximately 40 km wide, behind Tsushima Island. The low-transport zone is

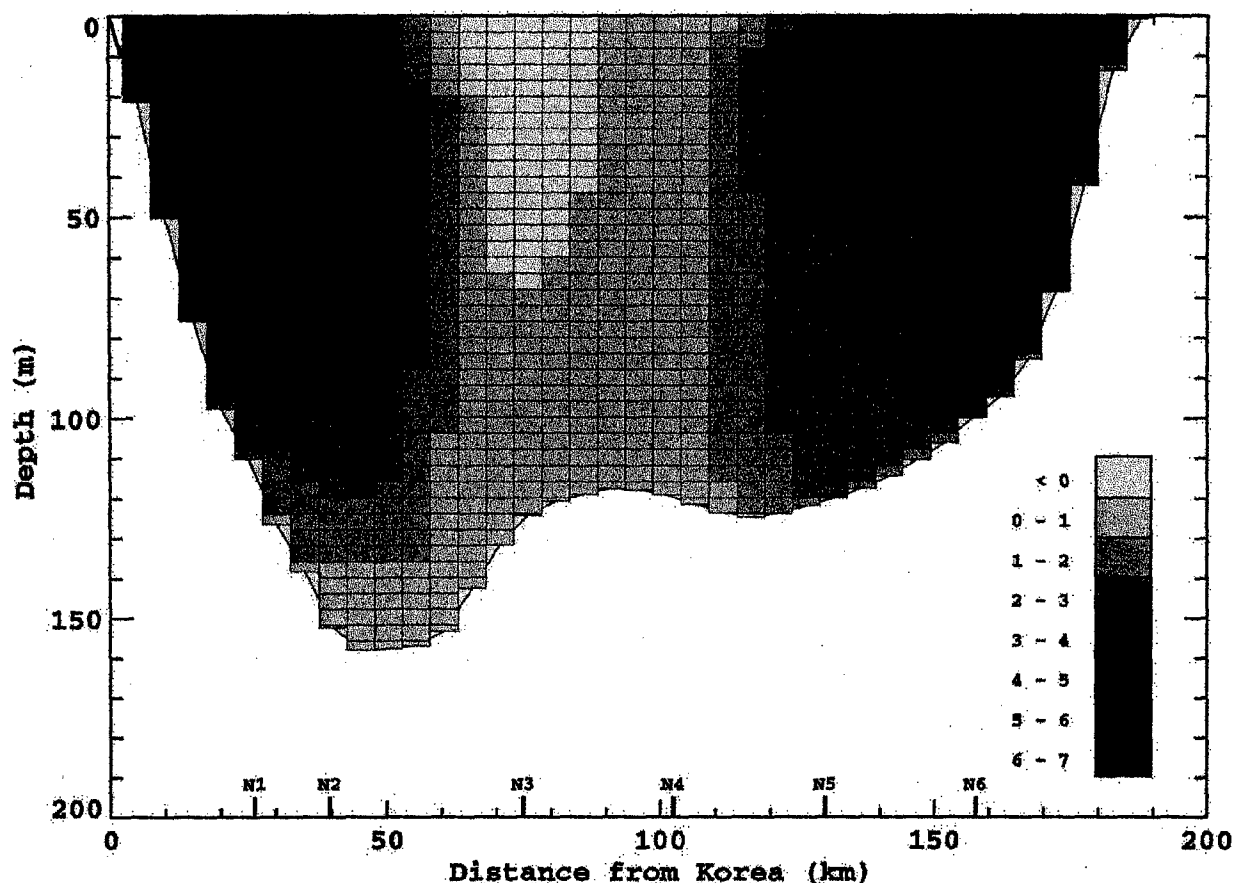


Fig. 5. As in Fig. 4 but for the north line.

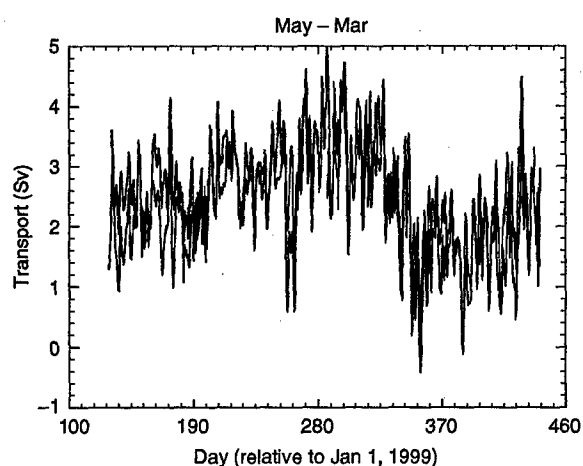


Fig. 6. Total transport estimates for the south line (thick line) and north line (thin line) are shown as a function of time.

shown by the thick bar located between N2 and N4 in Fig. 1. The middle of this low-transport zone is about 80 km from Korea. Therefore, all transport up to 80 km from Korea is assumed here to pass through the west channel, and all transport from 80 km off Korea to Japan is assumed to pass through the east channel.

Total transports for the north (2.38 Sv) and south (2.65 Sv) lines for May 1999–March 2000 should be nearly identical but differed by 0.27 Sv. As discussed above, the transport calculation for the south line is believed to be more accurate than the calculation for the north line. The western end of the north line is more likely to have a low calculated transport due to omission of intense currents often present near the Korean coast, as evidenced by the high velocities measured at N1

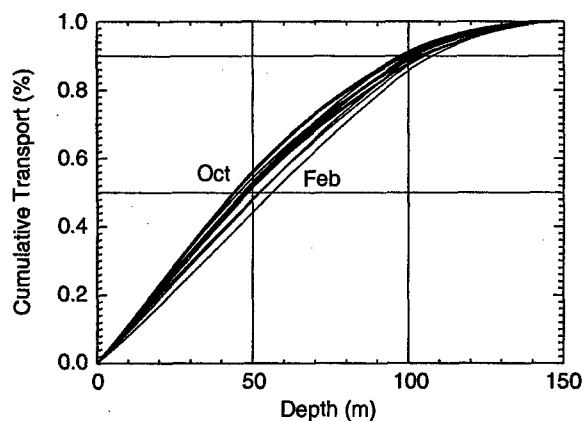


Fig. 7. Normalized cumulative transports versus depth for the southern line are shown for each month (thin lines, bounded by February and October) and for the 11-month average (thick line).

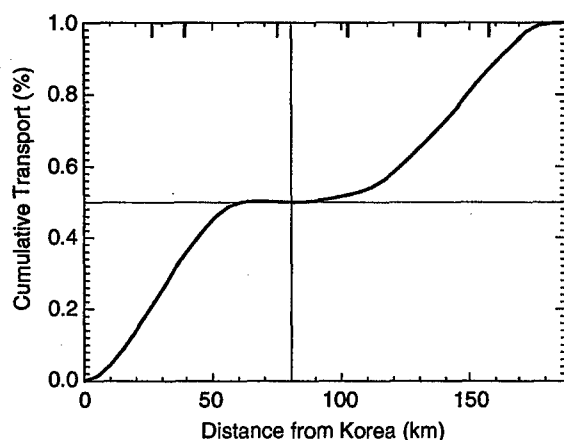


Fig. 8. Average cumulative transport distribution over the year as a function of distance from Korea for the north line. Positions of moorings, N1–N6, are indicated by the thick vertical bars on the top axis.

during the second half of the deployment period (N1 was not deployed during the first half of the deployment period). Therefore, the transport calculated for the eastern channel from the north line transport is considered more accurate than the transport calculated for the western channel. A better estimate of the transport for the western channel can be calculated using the transport through the south line. Transport through the

western channel is estimated from the difference of the total transport through the south line and the eastern channel transport. Thus, the total transport for the south line is then the sum of the west and east channel transports. Yearly and monthly transport totals for the south line, north line, west channel, and east channel are provided in Table 1. In general, total monthly mean transport is lowest in January (1.67 Sv) and then gradually increases to a maximum monthly mean value in October (3.59 Sv). In the west channel, minimum monthly mean transport occurs in December (0.77 Sv), while in the east channel, minimum monthly mean transport occurs in January (0.57 Sv). Maximum monthly mean transports for the west and east channels occur in October and are 2.02 and 1.57 Sv, respectively.

The additional coverage provided by N1, deployed closest to Korea from October 1999 to March 2000, does not make total transports through the north line agree more closely with total transports through the south line. Some of the worst agreements are found during February and March, while some of the better agreements are found during December and January. The main stream of the EKWC is located closest to the Korean coast in winter, while in summer, the EKWC is displaced farther from the coast and gradually becomes wider (Lie, 1984). Hence, best transport estimates at the north line are expected in summer, but this is not found to be the case

Table 1  
Korea/Tsushima Strait transports (Sv) for May 1999–March 2000

	South line	North line	West channel	East channel
May–Mar	2.65	2.38	1.46	1.19
May	2.69	1.97	1.38	1.31
Jun	2.78	2.22	1.61	1.17
Jul	2.70	2.32	1.56	1.14
Aug	3.01	2.92	1.45	1.56
Sep	3.03	2.82	1.70	1.33
Oct	3.59	3.32	2.02	1.57
Nov	3.05	3.29	1.67	1.38
Dec	1.83	1.91	0.77	1.06
Jan	1.67	1.57	1.10	0.57
Feb	2.09	1.53	1.27	0.82
Mar	2.75	2.16	1.52	1.23

here. Transports are actually larger for the north line than for the south line in the winter months of December and January.

The location along the south line where the transport splits into the western and eastern channels off Tsushima Island is generally near the middle of the strait but does vary. The variability in the location is shown in the cumulative transport distribution by month for the south line in Fig. 9. The thicker line is the mean cumulative transport over the 11 months and the thinner lines are the monthly distributions. The dashed vertical line is the average location, where

the total transport for the 11 months splits into west and east channels. The thin vertical line denotes the location where the monthly averaged transport must split to accommodate the east channel transport in the north line. The split location, about 31 km wide, is also shown by the thick bar located between S3 and S4 in Fig. 1. The average split location along the south line is 127 km from Korea ( $33.80^{\circ}\text{N}$ ,  $128.49^{\circ}\text{E}$ ), directly upstream from Tsushima Island. Monthly averaged transport distributions for March, and May–July (no measurements for April) closely approximate the 11-month transport average.

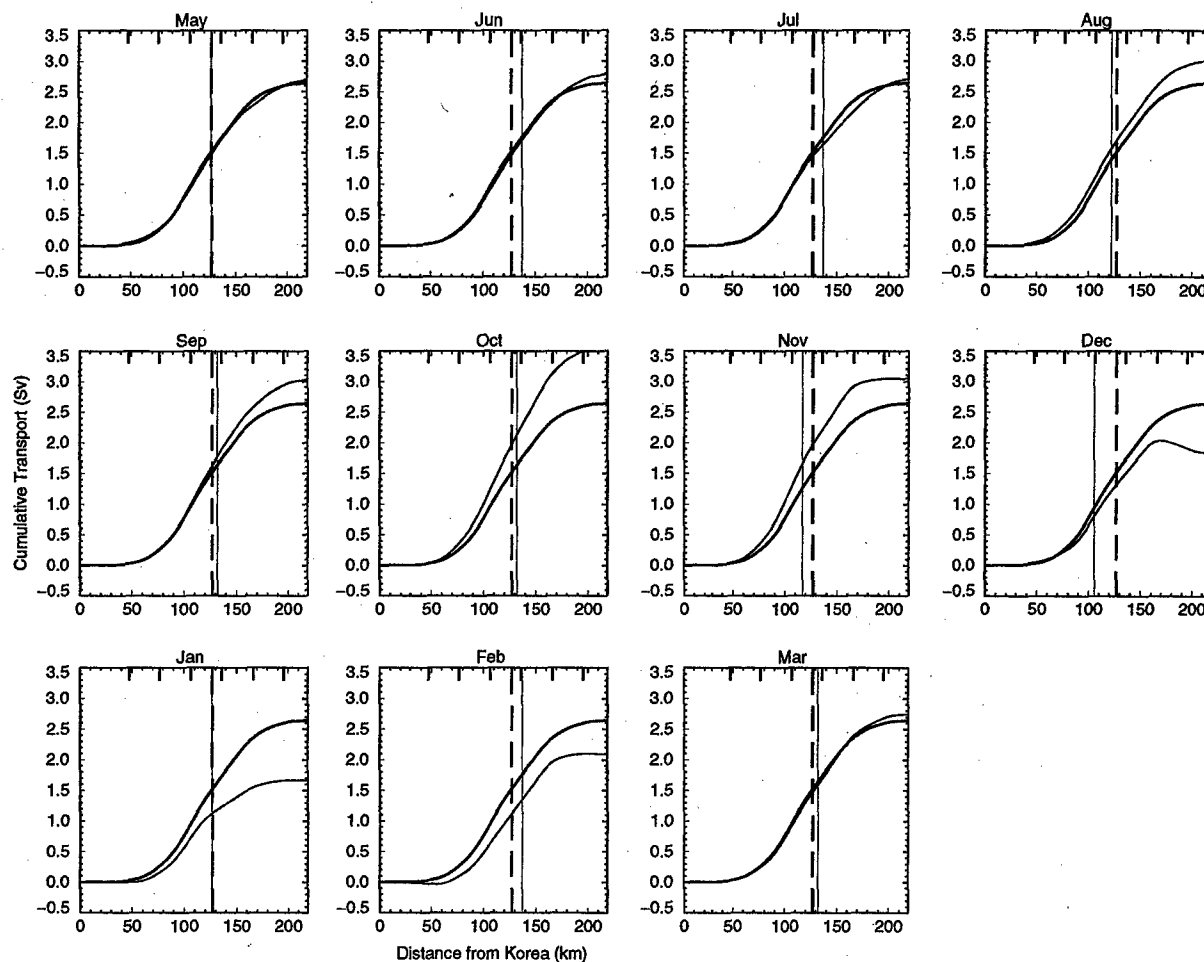


Fig. 9. Cumulative transport distributions for the south line are shown for the annual mean (thick line) and for each month (thin line). The dashed vertical line is the average location along the south line where the total transport for the 11 months splits into the west and east channels. The thin vertical line denotes the location where the monthly averaged transport must split. Positions of moorings, S1–S6, are indicated by the thick vertical bars on the top axes.

There does not appear to be a pattern in the split location in relation to transport larger and smaller than the 11-month mean. The split location for the lowest transport (January) is near the location of the split for the largest transport (October), and is located near the average split location. The average transport distribution across the Korea/Tsushima Strait ( $T^x$ ) along the south line, for 50 km to 195 km off Korea, can be approximated by

$$T^x = az^3 + bz^2 + cz + d, \quad (2)$$

where  $a = -1.770 \times 10^{-6}$ ,  $b = 6.372 \times 10^{-4}$ ,  $c = -4.954 \times 10^{-2}$ , and  $d = 1.129$ . The standard deviation of the observations with the fitted values is  $2.33 \times 10^{-2}$ .

The time-dependent transport distribution across the Korea/Tsushima Strait along the north line generally consists of outflow in the western and eastern channels, separated by a weak inflow or outflow region upstream of Tsushima Island. Representative transport cross-sections for the

north line are shown in Fig. 10. The most common scenario consists of a stronger transport in the western channel than in the eastern channel (Fig. 10c). This occurs about 61% of the time for this measurement period. Similar transports in the western and eastern channels occurs about 26% of the time (Figs. 10a and b), slightly stronger transport in the eastern channel occurs about 8% of the time. However, an apparent triple branching (Fig. 10d) is sometimes observed (5% of the time) in December and January. A triple branch structure is discussed by Kawai (1974) and Katoh (1994). In their triple branch scenario, the middle or Second Branch, referred to as the Offshore Branch, originates in the western channel along with the Third Branch, referred to as the East Korea Warm Current (Katoh, 1994). The middle and eastern transport outflow along the north line appear to originate in the eastern channel but could be caused by an eddy formed behind Tsushima Island and suggests that island wake dynamics influence the overall circulation patterns

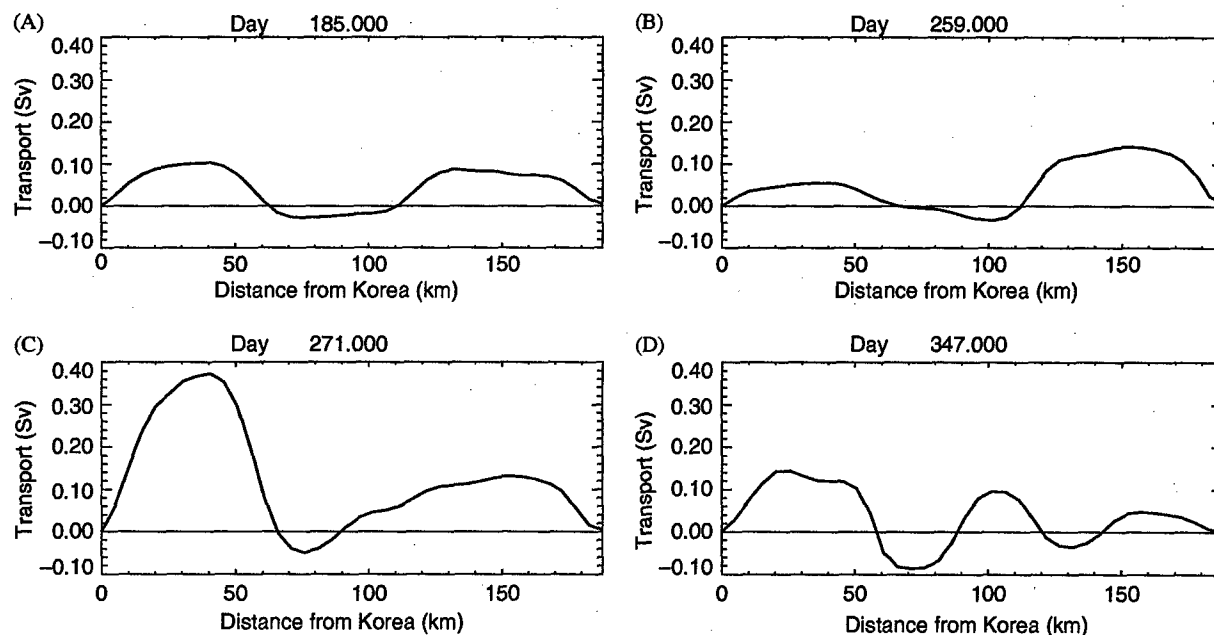


Fig. 10. Representative transport cross-sections for the north line: (A) transport similar in magnitude in the western and eastern channels (26% of the time), (B) transport stronger in the eastern channel than in the western channel (8% of the time), (C) transport stronger in the western channel than in the eastern channel (61% of the time), and (D) three outflows separated by weak inflow regions (5% of the time).

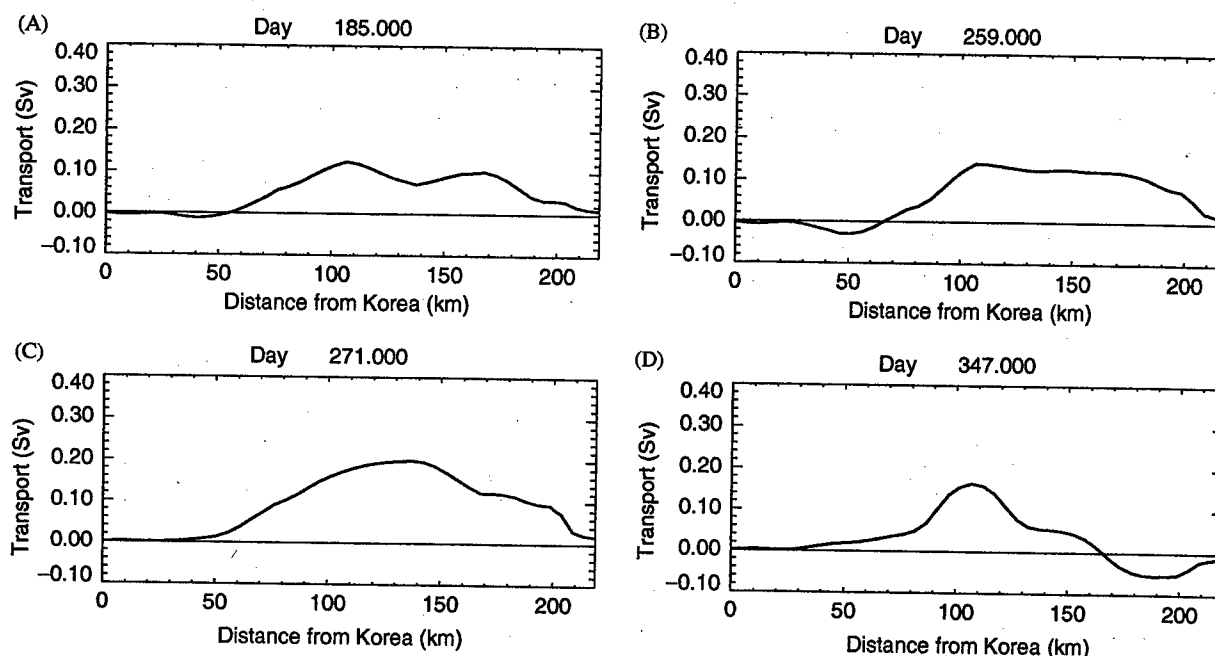


Fig. 11. Transport cross-sections for the south line, corresponding in time to the sections for the north line presented in Fig. 10.

downstream of Tsushima Island (see Section 5). The Offshore Branch is observed by Katoh (1994) to form further downstream.

The corresponding transports for the same days through the south line, upstream of the north line, are shown in Fig. 11. The most common transport distribution for the south line consists of a single, near mid-strait broad core (Fig. 11c) and commonly results in the stronger west channel flow (Fig. 10c). The somewhat flattened, twin peak, broad core (Fig. 11a) results in nearly an equal split in transport distribution between east and west channels (Fig. 10a). A more even distribution of transport from mid-strait to near Japan (Fig. 11b) results in a larger transport in the eastern channel (Fig. 11b). A strong counter transport near Japan and a weak transport near mid-strait (Fig. 11d) is typically located upstream of the triple core in the north line (Fig. 10d).

### 5. Tsushima Island wake

Understanding of island wake zones is important to the fishing industry since wakes and eddies

can trap suspended material and particles, and can accumulate plankton. In addition, wakes can greatly affect contaminant drifts. An island wake is located downstream of Tsushima Island throughout much of the measurement period and is likely a permanent feature. As illustrated in Figs. 2 and 3, the flow patterns across the Korea/Tsushima Strait downstream and upstream of the Tsushima Island are considerably different. The upstream pattern resembles a typical cross-channel current distribution expected from an open channel flow, with a jet feature near the surface in the middle of the channel (Fig. 2). In the downstream cross-section (Fig. 3), the core flow splits into two branches and the core of each branch is displaced toward the edge of the strait. The wake zone is indicated near the middle of the strait where a weak return flow is present for much of the measurement period at N3 and for several months at N4.

The flow pattern described above is also apparent in the daily transport data, shown in the three-dimensional space-time plot of transport both upstream and downstream of Tsushima Island in Fig. 12, and suggests that the

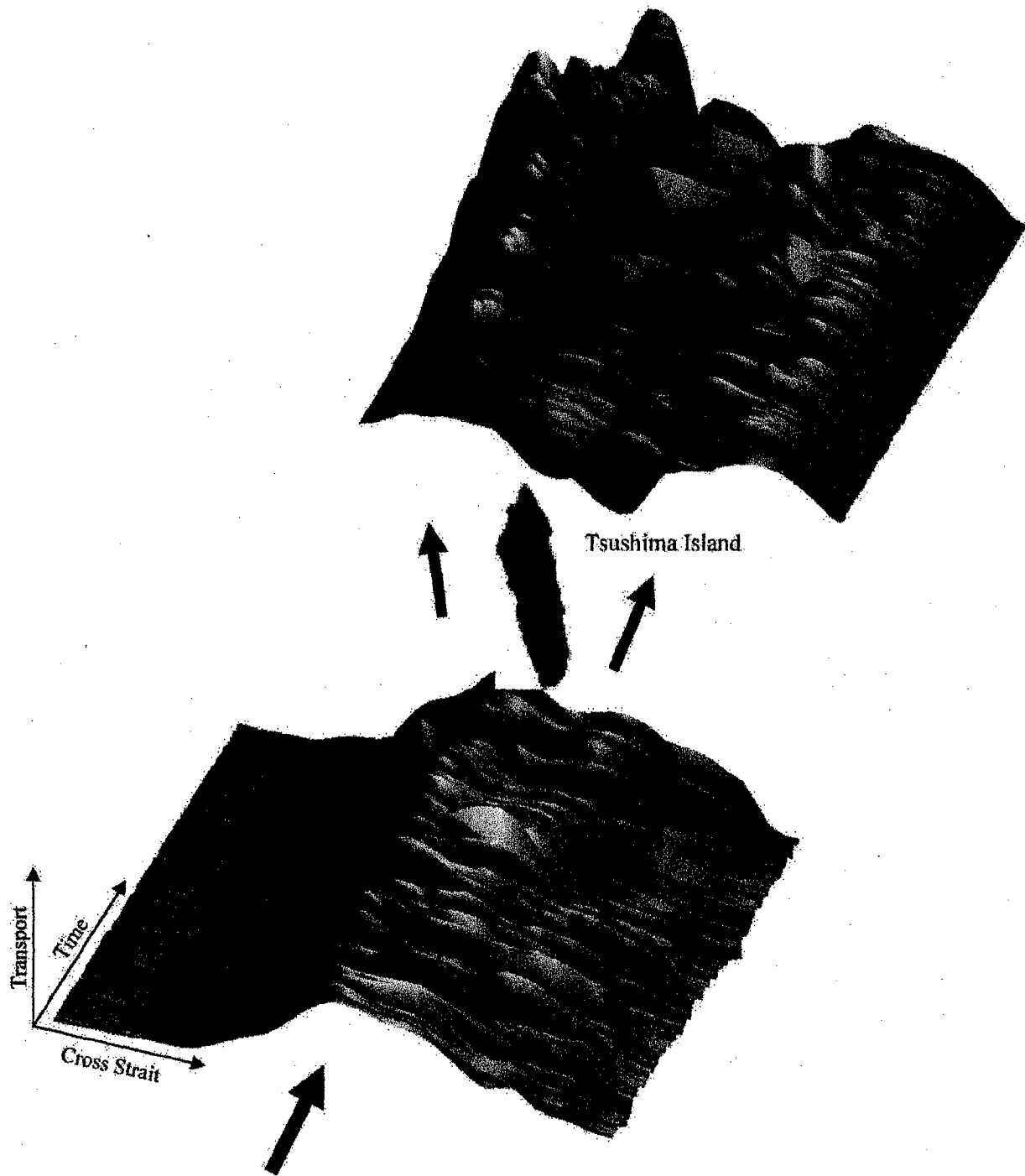


Fig. 12. Three-dimensional depiction of the transport upstream (along the south line) and downstream (along the north line) of Tsushima Island.



downstream wake pattern is a permanent presence at the instrument site about 100 km downstream from Tsushima Island. One of the interesting features of the downstream wake is its quasi-periodic fluctuation. This periodic fluctuation can be seen in the time series of the rotating current vectors at stations N3 and N4 (Figs. 13a and b). The period of the rotating current is estimated to be about a week. The persistent oscillatory pattern at the downstream of the Tsushima Island strongly suggests the occurrence of periodic shedding of eddies.

One of the earliest studies of eddy shedding by islands in the ocean is reported by Barkley (1972) around Johnston Atoll, a deep-ocean island

located about 100 km southwest of the Hawaii Islands. The island is roughly elliptical in shape with an equivalent diameter of 26 km. Based on long-line drift data, the drifts of two research ships, and Geomagnetic Electrokinetograph (GEK) measurements, he observed a Karman vortex street flow pattern downstream of the atoll in February 1968 when the mean current was about 0.60 m/s. The vortex pattern disappeared in the next visit during October 1968 when the flow was much weaker, with mean speed between 0.15 and 0.20 m/s.

Flow behavior behind obstacles (or islands) is characterized by the dimensionless Reynolds number  $Re$ , defined as the ratio of the inertial

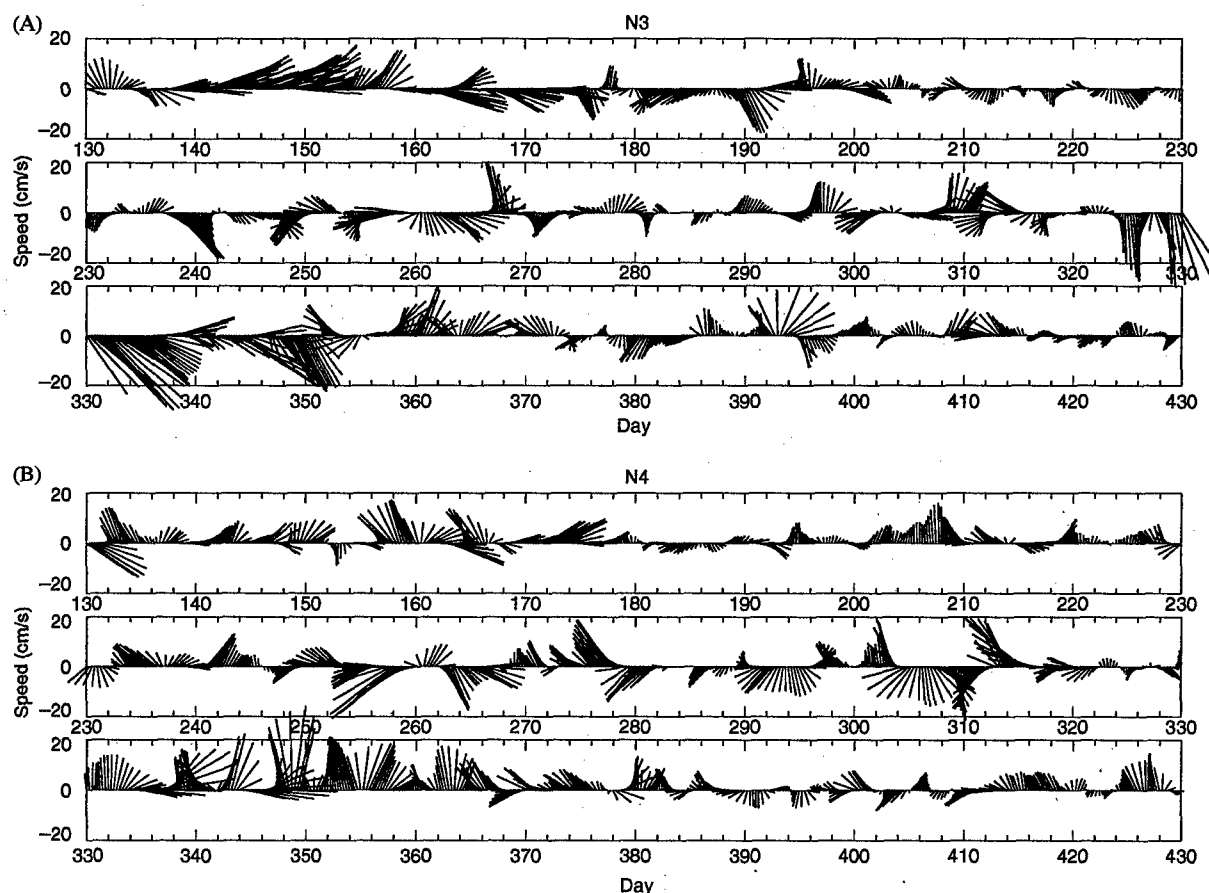


Fig. 13. The temporal history of the velocity vectors at 20 m depth for the downstream stations of (A) N3 and (B) N4. The velocities have been rotated so that positive vectors normal to the  $x$ -axis are directed along strait towards the Japan/East Sea. The periodic rotation of the velocity vectors strongly suggests continuous eddy shedding or periodic wakes.

force and the frictional force at the obstacle boundary (coast)

$$Re = \frac{U_0 L}{K}, \quad (3)$$

where  $U_0$  is the free-stream speed,  $L$  is the diameter of island, and  $K$  is the eddy viscosity. Using a value of  $220 \text{ m}^2/\text{s}$  as the eddy viscosity, the Reynolds number is 70 for the strong flow and 20 for the weaker flow conditions described above for the Johnston's Atoll. The threshold condition for vortex shedding is determined to be between these two Reynolds numbers (Barkley, 1972).

The frequency of the vortex shedding, expressed in non-dimensional form by the Strouhal number is given by

$$S = \frac{N_e L}{U_0}, \quad (4)$$

where  $N_e$  is the eddy frequency. The wavelength and period of the vortex street for Johnston's Atoll are 160 km and 4 days for the high-speed flow condition. The corresponding Strouhal number is 0.12. Barkley (1972) also compares the Johnston Atoll wake with the atmospheric wake observed downstream of Madeira (Chopra and Hubert, 1964, 1965) and demonstrates the close resemblance of the two wake systems. The prevalence of the Karman vortex street in the atmosphere downstream of islands have been continuously observed in satellite images (e.g., Castro et al., 2001).

Fig. 2 shows the temporal evolution of the daily mean velocity profiles at the six stations upstream of the Tsushima Island. During the months from May to mid-November, the core velocity (S2, S3, and S4) is generally higher than 0.2 m/s and can reach to 0.5 m/s in mid-September. In the winter time between December and February, the mean velocity is generally just above 0.1 m/s and rarely exceeds 0.25 m/s. Assuming that the horizontal eddy viscosity,  $K$ , of the Korea/Tsushima Strait is between 100 and  $200 \text{ m}^2/\text{s}$ , the representative Reynolds numbers range from 22 to 90 and Strouhal numbers range from 0.145 to 0.289 (Table 2). Effective diameter of the island of 30 km and eddy period of 8 days are assumed in these computations.

Table 2

Reynolds and Strouhal numbers representing the mean flow in the Korea/Tsushima Strait

$U$ (m/s)	$K$ ( $\text{m}^2/\text{s}$ )	$Re$	$S$
0.30	100	90.0	0.145
0.30	200	45.0	0.145
0.15	100	45.0	0.289
0.15	200	22.5	0.289

Tomczak (1988), citing Batchelor (1967), remarks that for a circular body, transition from fully attached flow to formation of an eddy pair occurs at a Reynolds number of around 1, periodic oscillation of the wake occurs at a Reynolds number around 35, and eddy shedding occurs at a Reynolds number around 65. The higher Reynolds numbers listed in Table 2 suggest that continuous eddy shedding can be expected downstream of the Tsushima Island in the months from May to November. For the rest of year periodic oscillating wakes or weak eddy shedding is most likely the dominant flow pattern. This scenario is consistent with the observed temporal evolution of the daily mean velocity profiles observed in the downstream stations (Fig. 3), especially at N3 and to a lesser extent at N4. Counter flows at N3 and N4 suggest eddy activity. Because eddies and wakes represent regions of strong energy sink, the region directly downstream of Tsushima Island is adverse to formation of current branching. Eddy formation just downstream of Tsushima Island can be misinterpreted as triple branching.

## 6. Summary and conclusions

From May 1999–March 2000, total average transport through the Korea/Tsushima Strait was 2.65 Sv, and average transports through the western and eastern channels were 1.46 and 1.19 Sv, respectively. Highest transports occur in fall and lowest transports occur in winter. Transport is more surface-intensified and depth-dependent in summer and fall than during winter and spring, where transports are nearly homogeneous over depth. Generally, about half of the transport

in the strait is contained in the upper 50 m, and about 10% of the transport is found below 100 m depth. Transport is greater in the western channel than in the eastern channel except during August and December. The Tsushima Current splits around Tsushima Island over a region about 31 km wide along the south line, on average about 127 km from Korea (33.80°N, 128.49°E). A wake zone, about 40 km wide, is located downstream of Tsushima Island and is a region of low transport and high variability. Eddy formation in the wake zone can give the false appearance of a triple branching just downstream of Tsushima Island. The island wake forms when transport is large and the wake zone actually prevents formation of a third branch at mid-strait.

### Acknowledgments

We thank Dr. Mark Wimbush of the Graduate School of Oceanography at the University of Rhode Island for his suggestion to apply island-wake theory in the Korea/Tsushima Strait. This work was sponsored by the Office of Naval Research (Program Element PE0601153N) as part of the basic research projects "Linkages of Asian Marginal Seas" and "Japan East Sea DRI" under Program Element 0601153N. This work is a contribution of the Naval Research Laboratory (NRL-SSC Contribution JA/7332-02-0053).

### References

- Barkley, R.A., 1972. Johnston Atoll's wake. *Journal of Marine Research* 30, 201–216.
- Batchelor, G.K., 1967. *An Introduction to Fluid Dynamics*. Cambridge University Press, Cambridge, pp. 515.
- Bretherton, F.P., Davis, R.E., Fandry, C.B., 1976. A technique for objective analysis and design of oceanographic experiments applied to MODE-73. *Deep-Sea Research* 23, 559–582.
- Castro, I., Vosper, S., Paisley, M., Hayden, P., 2001. Vortex shedding behind tapered obstacles in neutral stratified flow. *Dynamics of Atmospheres and Oceans* 34, 145–163.
- Cho, Y.-K., Kim, K., 1998. Structure of the Korea Strait Bottom Cold Water and its seasonal variation in 1991. *Continental Shelf Research* 18, 791–804.
- Choi, B.H., 1999. *Digital Atlas for Neighboring Seas of Korean Peninsula*. Laboratory for Coastal And Ocean Dynamics Studies, Sung Kyun Kwan University, CDRM.
- Chopra, K.P., Hubert, L.F., 1964. Karman vortex-streets in Earth's atmosphere. *Nature* 203, 1341–1343.
- Chopra, K.P., Hubert, L.F., 1965. Mesoscale eddies in wake of islands. *Journal of Atmospheric Science* 22, 652–657.
- Chang, K.-I., Suk, M.-S., Pang, I.-C., Teague, W.J., 2000. Observations of the Cheju Current. *Journal of Korean Society of Oceanography* 35, 129–152.
- Egawa, T., Nagata, Y., Sato, S., 1993. Seasonal variation of the Current in the Tsushima Strait deduced from ADCP data of ship-of-opportunity. *Journal of Oceanography* 49, 39–50.
- Isobe, A., 1997. The determinant of the volume transport distribution of the Tsushima Warm Current around the Tsushima/Korea Straits. *Continental Shelf Research* 17, 319–336.
- Isobe, A., Tawara, S., Kaneko, A., Kawano, M., 1994. Seasonal variability in the Tsushima Warm Current, Tsushima–Korea Strait. *Continental Shelf Research* 14, 23–35.
- Isobe, A., Ando, M., Watanabe, T., Senjyu, T., Sugihara, S., Manda, A., 2002. Freshwater and temperature transports through the Tsushima–Korea Straits. *Journal of Geophysical Research* 107 (C7) (art. no. 3065).
- Jacobs, G.A., Perkins, H.T., Teague, W.J., Hogan, P.J., 2001. Summer Transport Through the Korea–Tsushima Strait. *Journal of Geophysical Research* 106, 6917–6929.
- Kaneko, A., Byun, S.-K., Chang, S.-D., Takahashi, M., 1991. An observation of sectional velocity structures and transport of the Tsushima Current across the Korea Strait. In: Takano, K. (Ed.), *Oceanography of Asian Marginal Seas*. Elsevier, Amsterdam, pp. 179–195.
- Katoh, O., 1993. Detailed Current Structures in the Eastern Channel of the Tsushima Strait in Summer. *Journal of Oceanography* 49, 17–30.
- Katoh, O., 1994. Structure of the Tsushima Current in the Southwestern Japan Sea. *Journal of Oceanography* 50, 317–338.
- Katoh, O., Teshima, K., Kubota, K., Tsukiyama, K., 1996. Downstream transition of the Tsushima Current west of Kyushu in summer. *Journal of Oceanography* 52, 93–108.
- Kawabe, M., 1982. Branching of the Tsushima Current in the Japan Sea, Part I: Data analysis. *Journal of Oceanographic Society of Japan* 38, 95–107.
- Kawai, H., 1974. Transition of current images in the Japan Sea. In: *Japanese Society of Science and Fisheries* (Ed.), *The Tsushima Current–Oceanic Structure and Fishery*. Koseisha-Koseikaku, Tokyo, pp. 7–26 (in Japanese).
- Kawatate, K., Miita, T., Ouchi, Y., Mizuno, S., 1988. A report on failures of current meter moorings set east of Tsushima Island from 1983 to 1987. *Progress in Oceanography* 21, 319–327.
- Lee, C.K., 1974. The drift bottle experiment in the southern sea of Korea. *Bulletin of Fisheries Research and Development Agency* 12, 7–26 (in Korean with English abstract).
- Lie, H.-J., 1984. Coastal current and its variation along the east coast of Korea. In: Ichiye, T. (Ed.), *Ocean Hydrodynamics of the Japan and East China Seas*. Elsevier Oceanography Series 39, New York, pp. 399–408.

- Lie, H.-J., Cho, C.-H., Lee, J.-H., Lee, S., Tang, Y., 2000. Seasonal variation of the Cheju Warm Current in the northern East China Sea. *Journal of Oceanography* 56, 197–211.
- Lorenc, A.C., 1981. A global three-dimensional multivariate statistical interpolation scheme. *Monthly Weather Review* 109, 701–721.
- Miita, T., 1976. Transports of fish eggs and larvae in waters west of Kyushu. 2-2 Current structures observed by anchored measurements. *Bulletin of Japanese Society of Fisheries and Oceanography* 28, 33–58 (in Japanese).
- Miita, T., Ogawa, Y., 1984. Tsushima currents measured with current meters and drifters. In: Ichiye, T. (Ed.), *Ocean Hydrodynamics of the Japan and East China Seas*. Elsevier Oceanography Series 39, New York, pp. 67–76.
- Mizuno, S., Kawatate, K., Nagahama, T., Miita, T., 1989. Measurements of East Tsushima Current in winter and estimation of its seasonal variability. *Journal of the Oceanographic Society of Japan* 45, 375–384.
- Perkins, H., Teague, W.J., Jacobs, G.A., Chang, K.-I., Suk, M.-S., 2000a. Currents in Korea–Tsushima Strait During Summer 1999. *Geophysical Research Letters* 27 (19), 3033–3036.
- Perkins, H., de Strobel, F., Gualdesi, L., 2000b. The Barny Sentinel Trawl-resistant ADCP bottom mount: design, testing, and application. *IEEE Journal Oceanic Engineering* V25 (4), 430–436.
- Suda, K., Hidaka, K., 1932. The results of the oceanographical observations aboard R.M.S. Syunpu Maru in the southern part of the Sea of Japan in the summer of 1929, Part 1. *Journal of Oceanography Imperial Marine Observations* 3, 291–375 (in Japanese).
- Tawara, S., Fujiwara, T., 1985. Sea surface temperature distribution and its variability across the Tsushima Strait. *Journal of Oceanographic Society of Japan* 41, 49–55.
- Teague, W.J., Perkins, H.T., Hallock, Z.R., Jacobs, G.A., 1998. Current and tide observations in the southern Yellow Sea. *Journal Geophysical Research* 103, 27,783–27,793.
- Teague, W.J., Perkins, H.T., Jacobs, G.A., Book, J.W., 2001. Tide Observations in the Korea–Tsushima Strait. *Continental Shelf Research* 21, 545–561.
- Teague, W.J., Jacobs, G.A., Perkins, H.T., Book, J.W., Chang, K.-I., Suk, M.-S., 2002. Low frequency current observations in the Korea Strait. *Journal of Physical Oceanography*, 1621–1641.
- Toba, Y., Tomizawa, K., Kurasawa, Y., Hanawa, K., 1982. Seasonal and year-to-year variability of the Tsushima–Tsugaru Warm Current system with its possible cause. *La Mer* 20, 41–51.
- Tomczak, M., 1988. Island wakes in deep and shallow water. *Journal of Geophysical Research* 93, 5153–5154.
- Uda, M., 1934. The results of simultaneous oceanographical investigations in the Japan Sea and its adjacent waters in May and June, 1932. *Japan Imperial Fishery Experimental Stations* 5, 57–190 (in Japanese).
- Yi, S.U., 1966. Seasonal and secular variations of the water volume transport across the Korea Strait. *Journal of Oceanological Society of Korea* 1, 7–13.
- Yi, S.U., 1970. Variations of oceanic condition and mean sea level in the Korea Strait. In: Marr, J.C. (Ed.), *The Kuroshio (A symposium on the Japan current)*. East-West Center Press, pp. 125–141.
- Yoon, J.H., 1982a. Numerical experiment on the circulation in the Japan Sea, Part 1: formation of the East Korean Warm Current. *Journal of Oceanographic Society of Japan* 38, 38–43.
- Yoon, J.H., 1982b. Numerical experiment on the circulation in the Japan Sea, Part 3: mechanism of the nearshore branch of the Tsushima Current. *Journal of Oceanographic Society of Japan* 38, 125–130.